

## Special Issue: Polymers for Microelectronics

**Guest Editors:** Dr Brian Knapp (Promerus LLC) and  
Prof. Paul A. Kohl (Georgia Institute of Technology)

### EDITORIAL

#### Polymers for Microelectronics

B. Knapp and P. A. Kohl, *J. Appl. Polym. Sci.* 2014, DOI: [10.1002/app.41233](https://doi.org/10.1002/app.41233)

### REVIEW

#### Negative differential conductance materials for flexible electronics

A. Nogaret, *J. Appl. Polym. Sci.* 2014, DOI: [10.1002/app.40169](https://doi.org/10.1002/app.40169)

### RESEARCH ARTICLES

#### Generic roll-to-roll compatible method for insolubilizing and stabilizing conjugated active layers based on low energy electron irradiation

M. Helgesen, J. E. Carlé, J. Helt-Hansen, A. Miller, and F. C. Krebs, *J. Appl. Polym. Sci.* 2014, DOI: [10.1002/app.40795](https://doi.org/10.1002/app.40795)

#### Selective etching of polylactic acid in poly(styrene)-block-poly(D,L)lactide diblock copolymer for nanoscale patterning

C. Cummins, P. Mokarian-Tabari, J. D. Holmes, and M. A. Morris, *J. Appl. Polym. Sci.* 2014, DOI: [10.1002/app.40798](https://doi.org/10.1002/app.40798)

#### Preparation and dielectric behavior of polyvinylidene fluoride composite filled with modified graphite nanoplatelet

P. Xie, Y. Li, and J. Qiu, *J. Appl. Polym. Sci.* 2014, DOI: [10.1002/app.40229](https://doi.org/10.1002/app.40229)

#### Design of a nanostructured electromagnetic polyaniline–Keggin iron–clay composite modified electrochemical sensor for the nanomolar detection of ascorbic acid

R. V. Lilly, S. J. Devaki, R. K. Narayanan, and N. K. Sadanandhan, *J. Appl. Polym. Sci.* 2014, DOI: [10.1002/app.40936](https://doi.org/10.1002/app.40936)

#### Synthesis and characterization of novel phosphorous-silicone-nitrogen flame retardant and evaluation of its flame retardancy for epoxy thermosets

Z.-S. Li, J.-G. Liu, T. Song, D.-X. Shen, and S.-Y. Yang, *J. Appl. Polym. Sci.* 2014, DOI: [10.1002/app.40412](https://doi.org/10.1002/app.40412)

#### Electrical percolation behavior and electromagnetic shielding effectiveness of polyimide nanocomposites filled with carbon nanofibers

L. Nayak, T. K. Chaki, and D. Khastgir, *J. Appl. Polym. Sci.* 2014, DOI: [10.1002/app.40914](https://doi.org/10.1002/app.40914)

#### Morphological influence of carbon modifiers on the electromagnetic shielding of their linear low density polyethylene composites

B. S. Villacorta and A. A. Ogale, *J. Appl. Polym. Sci.* 2014, DOI: [10.1002/app.41055](https://doi.org/10.1002/app.41055)

#### Electrical and EMI shielding characterization of multiwalled carbon nanotube/polystyrene composites

V. K. Sachdev, S. Bhattacharya, K. Patel, S. K. Sharma, N. C. Mehra, and R. P. Tandon, *J. Appl. Polym. Sci.* 2014, DOI: [10.1002/app.40201](https://doi.org/10.1002/app.40201)

#### Anomalous water absorption by microelectronic encapsulants due to hygrothermal-induced degradation

M. van Soestbergen and A. Mavinkurve, *J. Appl. Polym. Sci.* 2014, DOI: [10.1002/app.41192](https://doi.org/10.1002/app.41192)

#### Design of cyanate ester/azomethine/ZrO<sub>2</sub> nanocomposites high-k dielectric materials by single step sol-gel approach

M. Ariraman, R. Sasi Kumar and M. Alagar, *J. Appl. Polym. Sci.* 2014, DOI: [10.1002/app.41097](https://doi.org/10.1002/app.41097)

#### Furan/imide Diels–Alder polymers as dielectric materials

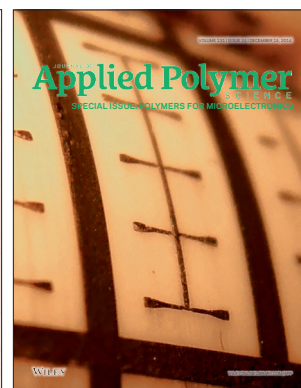
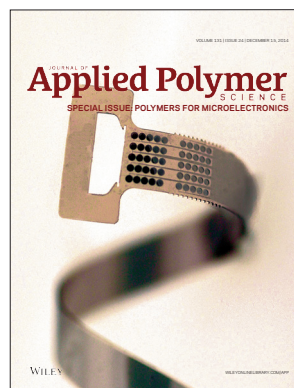
R. G. Lorenzini and G. A. Sotzing, *J. Appl. Polym. Sci.* 2014, DOI: [10.1002/app.40179](https://doi.org/10.1002/app.40179)

#### High dielectric constant polyimide derived from 5,5'-bis[(4-amino) phenoxy]-2,2'-bipyrimidine

X. Peng, Q. Wu, S. Jiang, M. Hanif, S. Chen, and H. Hou, *J. Appl. Polym. Sci.* 2014, DOI: [10.1002/app.40828](https://doi.org/10.1002/app.40828)

#### The influence of rigid and flexible monomers on the physical-chemical properties of polyimides

T. F. da Conceição and M. I. Felisberti, *J. Appl. Polym. Sci.* 2014, DOI: [10.1002/app.40351](https://doi.org/10.1002/app.40351)



## Special Issue: Polymers for Microelectronics

**Guest Editors:** Dr Brian Knapp (Promerus LLC) and  
Prof. Paul A. Kohl (Georgia Institute of Technology)

### Development of polynorbornene as a structural material for microfluidics and flexible BioMEMS

A. E. Hess-Dunning, R. L. Smith, and C. A. Zorman, *J. Appl. Polym. Sci.* 2014, DOI: [10.1002/app.40969](https://doi.org/10.1002/app.40969)

### A thin film encapsulation layer fabricated via initiated chemical vapor deposition and atomic layer deposition

B. J. Kim, D. H. Kim, S. Y. Kang, S. D. Ahn, and S. G. Im, *J. Appl. Polym. Sci.* 2014, DOI: [10.1002/app.40974](https://doi.org/10.1002/app.40974)

### Surface relief gratings induced by pulsed laser irradiation in low glass-transition temperature azopolysiloxanes

V. Damian, E. Resmerita, I. Stoica, C. Ibanescu, L. Sacarescu, L. Rocha, and N. Hurduc, *J. Appl. Polym. Sci.* 2014, DOI: [10.1002/app.41015](https://doi.org/10.1002/app.41015)

### Polymer-based route to ferroelectric lead strontium titanate thin films

M. Benkler, J. Hobmaier, U. Gleißner, A. Medesi, D. Hertkorn, and T. Hanemann, *J. Appl. Polym. Sci.* 2014, DOI: [10.1002/app.40901](https://doi.org/10.1002/app.40901)

### The influence of dispersants that contain polyethylene oxide groups on the electrical resistivity of silver paste

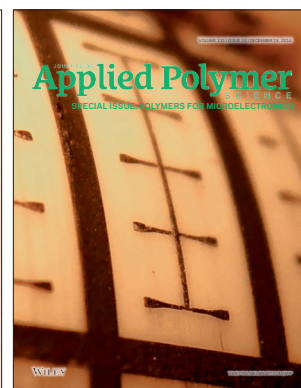
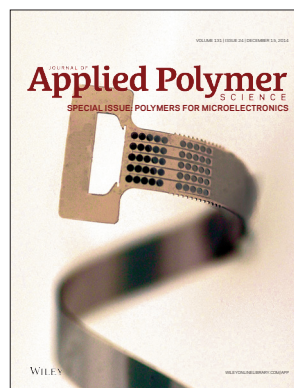
T. H. Chiang, Y.-F. Chen, Y. C. Lin, and E. Y. Chen, *J. Appl. Polym. Sci.* 2014, DOI: [10.1002/app.41183](https://doi.org/10.1002/app.41183)

### Quantitative investigation of the adhesion strength between an SU-8 photoresist and a metal substrate by scratch tests

X. Zhang, L. Du, and M. Zhao, *J. Appl. Polym. Sci.* 2014, DOI: [10.1002/app.41108](https://doi.org/10.1002/app.41108)

### Thermodynamic and kinetic aspects of defectivity in directed self-assembly of cylinder-forming diblock copolymers in laterally confining thin channels

B. Kim, N. Laachi, K. T. Delaney, M. Carilli, E. J. Kramer, and G. H. Fredrickson, *J. Appl. Polym. Sci.* 2014, DOI: [10.1002/app.40790](https://doi.org/10.1002/app.40790)



## The Influence of Rigid and Flexible Monomers on the Physical-Chemical Properties of Polyimides

Thiago Ferreira da Conceição, Maria Isabel Felisberti

Department of Physical Chemistry, Institute of Chemistry, University of Campinas (UNICAMP), P.O. Box 6154, Campinas, São Paulo 13083-970, Brazil

Correspondence to: M. I. Felisberti (E-mail: misabel@iqm.unicamp.br)

This article presents the synthesis and characterization of polyimides and copolyimides derived from rigid [4,4'-(9-fluorenylidene)dianiline (FNDA) and 3,3',4,4'-biphenyltetracarboxylic dianhydride (BPDA)] and flexible segments [4,4'-(1,3-phenylenedioxy) dianiline (PDODA) and ethylenediaminetetraacetic dianhydride (EDTAn)], by polyaddition followed by thermal imidization of the polyamic acid. It describes the characterization of the polyimides and the polyamic acids in accordance to <sup>1</sup>H NMR, FTIR, GPC, and XRD analysis, as well as solubility, mechanical (DMTA and stress–strain tests), thermal (DSC and TGA), and electric properties. Among the homopolymers, FNDA–BPDA and PDODA–BPDA form free-standing films. The first presents higher  $T_g$ , thermal stability and Young's modulus. To tailor the properties copolyimides of FNDA, PDODA, and BPDA were synthesized. Young's modulus,  $T_g$ , thermal stability, dielectric constant, and solubility progressively increase with increasing amount of FNDA. © 2014 Wiley Periodicals, Inc. *J. Appl. Polym. Sci.* **2014**, *131*, 40351.

**KEYWORDS:** dielectric properties; mechanical properties; polyimides; synthesis and processing; thermal properties

Received 14 November 2013; accepted 24 December 2013

DOI: 10.1002/app.40351

### INTRODUCTION

The development of new materials for high temperature applications is one prerequisite to the further development of high technology aircraft, satellites, defense artifacts, memories, and processors for the computer industry and in many other fields.<sup>1,2</sup> Among the available materials, polymers offer some unique advantages such as low density (of special interest for aerospace and automotive industries), low dielectric constant (of great importance for the electronic industry), and better corrosion resistance and tenacity, as compared to metals and ceramics, respectively. The class of polymers that is in the leading position in this segment is the aromatic polyimides, which are commercially available under a variety of trademarks. The most known and studied ones are Ultem®, Kapton®, and Uplex®, commercialized by DuPont, Sabic Innovative Plastics and Ube Industries, respectively. The type of products made of polyimides range from adhesive tapes to structural components (rods, sheets, and tubes) but films represent the biggest end use.<sup>3,4</sup> The use of polyimides as coatings for electrical wire insulation and corrosion protection has also attracted scientific attention.<sup>5–9</sup> To fulfill the needs of all these different technological fields this class of polymer must be able to be processed by a conventional thermomechanical processing (e.g., extrusion) or by solvent casting and still perform well at high temperatures, which represents a significant challenge for most polyimides.

Ultem® and Kapton® represent the standard melt processable and “infusible” polyimides, respectively, and they are usually taken as

references for the performance of new ones.<sup>3,4</sup> While the former has a  $T_g$  of 215°C, is soluble in organic solvents and thermo moldable, the latter has a  $T_g$  close to 400°C and must be processed as the precursor polyamic acid (in solution) since it is not soluble in any known solvent and infusible.<sup>4</sup> The better processability of Ultem® is related to the presence of the “bisphenol A” segment on its structure, which has two ether linkages that increase chain mobility and polarity, and an isopropylidene moiety, which increases the free volume.<sup>4</sup> The price to be paid for the better processability of Ultem® is its lower thermal stability, while for Kapton® (which is based on pyromellitic anhydride and oxydianiline) the higher thermal stability comes at the cost of lower processability. Attempts to reach the middle point in this equation “processability/thermal stability” have resulted in the synthesis of different polyimides with a variety of monomer structures.<sup>3,10</sup> The aim of this article is to contribute to the development of polyimides, which combine high thermal stability with good processability by investigating the influence of certain flexible and rigid monomers on polyimide properties. Special emphasis is given to polyimides films, which were characterized by means of electrochemical impedance spectroscopy and stress–strain tests.

### EXPERIMENTAL

#### Materials

N-Methyl-2-pyrrolidone (NMP) and acetone were purchased from Synth Chemicals and triethylamine (TEA) was obtained

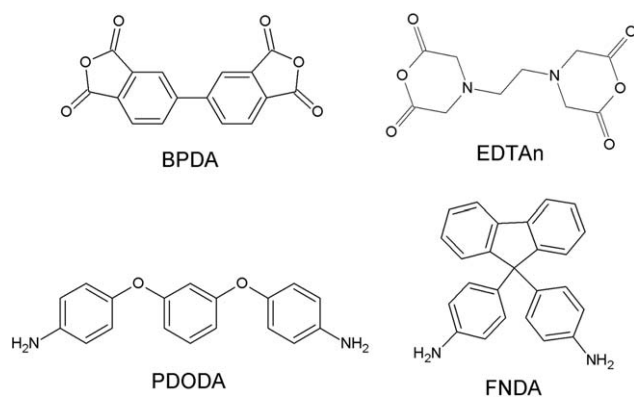


**Figure 1.** Monomers studied in this research.

from Tedia. The diamines 4,4'-(9-fluorenylidene) dianiline (FNDA) and 4,4'-(1,3-phenylenedioxy)dianiline (PDODA) and the dianhydrides 3,3',4,4'-biphenyltetracarboxylic dianhydride (BPDA) and ethylenediaminetetraacetic dianhydride (EDTAn) were obtained from Sigma Aldrich. The chemical structures of these monomers are shown in Figure 1. The solvent NMP was distilled under reduced pressure before each synthesis to assure its dryness and purity. The first and last fractions were discarded and the distillate was stored under dry nitrogen. PDODA was purified by recrystallization from ethanol solution, and then dried at room temperature under vacuum for several days, until no mass variation was observed. FNDA (99% of purity) was dried under vacuum for 12 h before use. The dianhydrides were dried under vacuum at high temperatures (150°C for BPDA and 130°C for EDTAn) for at least 20 h to assure dryness and that the carboxylic acid units were converted to the corresponding anhydride. Polyetherimide (PEI) (trade name ULTEM®1010) supplied by SABIC Innovative Plastics was used for comparison of the films mechanical properties.

### Synthesis of the Polymers

The syntheses of the polyimides and copolyimides were performed by the typical two step procedure: synthesis of polyamic acid and subsequent thermal imidization.<sup>4</sup> Table I shows the nomenclature and compositions of the polymers. Although the homopolyimides named as PDODA–BPDA and FNDA–BPDA have been described in the literature, we show here a detailed spectroscopic, mechanical, thermal, and dielectric characterization of them and their films.<sup>11–14</sup> From our knowledge the other polymers are reported here for the first time.

For the synthesis, equimolar amounts of diamine and dianhydride were dissolved in 15 mL of NMP to form a 28 wt % solution. The diamine was dissolved first, and then the dianhydride was added in equimolar amount. This sequence is important to avoid excess of dianhydride in the solution, which inhibits molar mass increase. For the copolyimides, FNDA and PDODA diamines were dissolved and mixed together for about 5 min, and then equimolar amount of BPDA was added to the solution.

The reaction medium was stirred under a dry N<sub>2</sub> atmosphere at room temperature for 3 h to form the corresponding polyamic acid. Considerable viscosity increase was observed after 1 h and

**Table I.** Molar Mass and Polydispersity of the Prepared Polyimides and Copolyimides

| Polymer                   | Polyimide                | M <sub>w</sub> (Da) | Polydispersity |
|---------------------------|--------------------------|---------------------|----------------|
| Polyimides                | PDODA-BPDA               | 7100                | 1.7            |
|                           | PDODA-EDTAn <sup>a</sup> | -                   | -              |
|                           | FNDA-BPDA                | 22,000              | 2.3            |
|                           | FNDA-EDTAn               | 11,000              | 1.8            |
| Copolyimides <sup>b</sup> | PD20FN <sup>a</sup>      | -                   | -              |
|                           | PD40FN                   | 14,000              | 1.9            |
|                           | PD50FN                   | 9000                | 1.6            |

<sup>a</sup> Molar mass of these polyimides could not be determined by GPC due to their low solubility in the salt or imidized form.

<sup>b</sup> PD, PDODA; XYFN, mol % of FNDA. The dianhydride used for the copolyimides synthesis was BPDA.

5 mL of NMP was added twice to reduce it. Triethylamine was then added in an equimolar amount to the acid groups, to form the quaternary ammonium salt. The conversion of polyamic acid to the salt was performed since the literature reports the higher stability of the salt in comparison to the acid.<sup>15,16</sup> The solution was further stirred for 2 h to complete this reaction. Then, the polyamic salt solution was diluted with NMP and the polymer was precipitated with acetone. The polymers were further washed with ethanol and acetone and then dried under vacuum at 80°C for several days.

### Film Preparation

Films of the polymers were prepared by solution casting. The polymers were dissolved in NMP to form a 25 wt % solution of high viscosity. The solutions were poured onto a glass plate at 65°C and spread over it using a spacer to control the wet thickness. The films were dried at this temperature for 5 h and then placed inside a vacuum oven at 165°C for a preimidization process. After this step, the films were removed from the plate and placed inside an oven, which was heated from 150 to 300°C at 1°C min<sup>-1</sup>, under N<sub>2</sub> and maintained at 300°C for 10 min. The imidized films, with 0.05 mm thicknesses, were then stored under dry conditions for further characterization.

### Polymer and Film Characterizations

All the polymers were characterized by <sup>1</sup>H nuclear magnetic resonance (<sup>1</sup>H NMR) (Bruker spectrophotometer, 200 MHz, in DMF-d<sub>7</sub>) and Fourier-transform infrared spectroscopy (FTIR) (spectrophotometer Bomem/MB-Series, 16 scans with 4 cm<sup>-1</sup> resolution) to confirm their chemical structure. The NMR analyses were performed on the salts, unless otherwise specified. The molar mass and its distribution were also determined for the polymers in the salt form, by gel permeation chromatography (GPC) (Viscotek GPCMax, VE 2001) using dimethylformamide (DMF) with UV detector and polystyrene standards. The thermal properties were investigated by thermogravimetric analyses (TGA) (TA instruments, TGA 2050 EGA furnace) under an argon atmosphere at a heating rate of 10°C min<sup>-1</sup>, from room temperature to 950°C, and differential scanning calorimetry (DSC) (TA instruments DSC 2910). In the DSC analyses the first run was performed from room temperature to 300°C, at a

heating rate of  $20^{\circ}\text{C min}^{-1}$ , to ensure dryness and imidization of the polymers, then the samples were cooled at this same rate to  $0^{\circ}\text{C}$  and finally, heated from  $0$  to  $350^{\circ}\text{C}$  at  $10^{\circ}\text{C min}^{-1}$  for the determination of the polymer glass transition temperature ( $T_g$ ). The  $T_g$  and secondary relaxations were also investigated by dynamic mechanical analyses (DMTA V Rheometric Scientific) on the polymer films, from  $-150$  to  $500^{\circ}\text{C}$  (depending on the polymer), with a frequency of  $1$  Hz, and a strain of  $0.2\%$  in a strain-compression mode. Analyses above  $400^{\circ}\text{C}$  were performed under argon. The X-ray diffractograms were obtained by XRD analyses on the polymer powders (Shimadzu XRD7000) using a wavelength of  $1.54 \text{ \AA}$  (Cu anode) in diffraction angles  $2\theta$  ranging from  $5^{\circ}$  to  $50^{\circ}$ .

The films mechanical properties were determined using the stress-strain mechanical tests according to ASTM D-882-09 performed on an EMIC universal machine. Imidized films of  $0.05 \times 10 \times 130 \text{ mm}^3$  dimensions were tested at an initial distance of  $100 \text{ mm}$  and at a speed of  $50 \text{ mm min}^{-1}$   $25^{\circ}\text{C}$  and  $50\%$  relative humidity. The dielectric constant of the films was obtained by means of electrochemical impedance spectroscopy performed in a Frequency Response Analyzer from  $10^2$  to  $10^5$  Hz at a perturbation of  $35 \text{ mV}$  over the rest potential, using parallel circular electrodes of  $1 \text{ cm}$  diameter. The dielectric constant was calculated from the impedance data in according to the method described in the Ref. 17.

## RESULTS AND DISCUSSION

### General Properties

The polymers were precipitated in acetone in the salt form, forming a white (in a few cases, slightly green) powder. All polymer salts are soluble in NMP. The salts of EDTAn based polymers are even soluble in water, especially PDODA-EDTAn. After imidization, however, FNDA-BPDA, PD50FN, and FNDA-EDTAn remain soluble in NMP while the other polymers become insoluble in the tested solvents (NMP, DMF,  $\text{CH}_2\text{Cl}_2$ , and THF). Table I shows the mass average molar mass ( $M_w$ ) and the polydispersity of the polymers (PDODA-EDTAn and PD20FN show low solubility in DMF in the salt and in the imidized form, therefore their molar mass was not determined). The molar masses ranged from  $7000$  to  $20000 \text{ Da}$  and the polydispersities were close to  $2$  in all cases, as expected for polycondensation polymers. All syntheses yielded more than  $95\%$  of product.

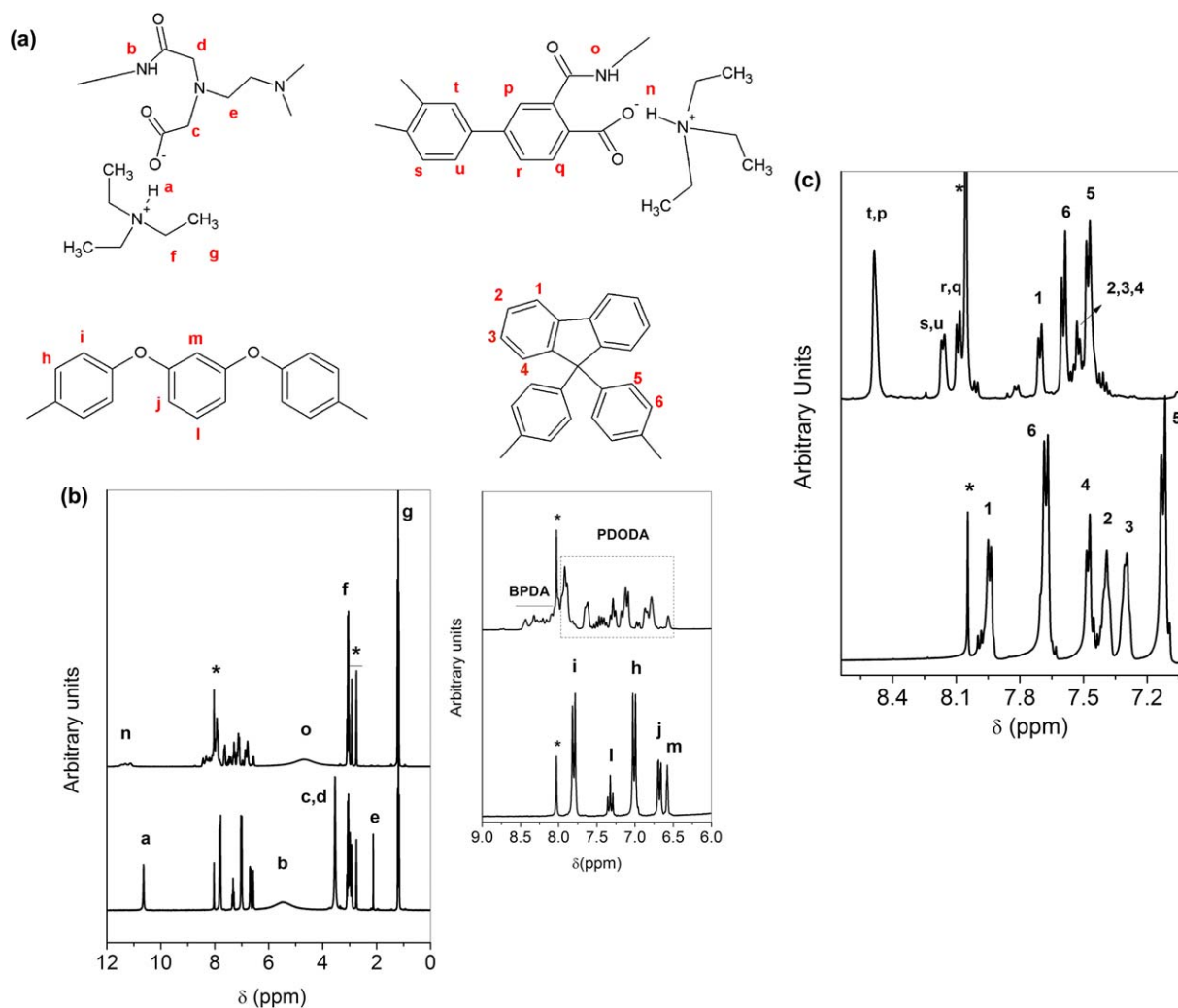
### Spectroscopic Characterization of the Polyimides

Figure 2 shows the  $^1\text{H}$  NMR spectra of the polyamic salts and the assignment of the main signals. In the following discussion, the hydrogens are named according to the assignments shown in Figure 2(a). In Figure 2(b), the full range  $^1\text{H}$  NMR spectra of PDODA polymers is shown, where the signals related to triethylamine [ $1.19 \text{ ppm}$  ( $\text{H}_g$ ) and  $3.03 \text{ ppm}$  ( $\text{H}_f$ )], to aromatic hydrogens (between  $6.0$  and  $8.5 \text{ ppm}$ ) and to the opened anhydride ring [amidic ( $\text{H}_b$ ,  $\text{H}_o$ ) and acid hydrogens ( $\text{H}_a$ ,  $\text{H}_n$ )] can be observed. The chemical shifts for the amidic and acid hydrogens are influenced by the structure of the anhydride [ $4.65 \text{ ppm}$  ( $\text{H}_o$ ) and  $11.23 \text{ ppm}$  ( $\text{H}_n$ ) for PDODA-BPDA and  $5.48 \text{ ppm}$  ( $\text{H}_b$ ) and  $10.64 \text{ ppm}$  ( $\text{H}_a$ ) for PDODA-EDTAn, respectively]. The higher acidity of the acid hydrogen in the case of PDODA-

BPDA is an expected result, which is related to the conjugated aromatic rings that produce a strong electron withdrawing effect. The higher acidity of the amidic hydrogen in the case of PDODA-EDTAn, as compared to PDODA-BPDA, is due to a stronger resonance effect of the nitrogen lone pair with the carbonyl group, resulting in this hydrogen being more deshielded. In PDODA-BPDA this resonance is weakened due to the competing conjugation of the carbonyl group with the aromatic ring of BPDA. The signals for the aliphatic carbons related to the reacted EDTAn moiety appear at  $3.54 \text{ ppm}$  ( $\text{H}_d$ ) and  $2.12 \text{ ppm}$  ( $\text{H}_e$ ). The inset in Figure 2(b) shows the aromatic region for these two polyimides. It can be observed that the spectrum of PDODA-EDTAn (bottom) is more well defined than that of PDODA-BPDA (top). This is related to the flexibility of the EDTAn segment, which might place the salt group ( $\text{COO}^- + \text{NH}(\text{CH}_2\text{CH}_3)_3$ ) away from the aromatic ring, inhibiting the anisotropic effect of the carbonyl.<sup>18</sup> For PDODA-EDTAn [Figure 2(b), bottom] the signals of PDODA can be clearly assigned (a singlet as the most shielded aromatic signal at  $6.58 \text{ ppm}$  ( $\text{H}_m$ ), only one triplet centered at  $7.33 \text{ ppm}$  ( $\text{H}_i$ ), related to the proton in the meta position to the oxygens in the biphenyl moiety, and three doublets at  $6.68 \text{ ppm}$  ( $\text{H}_j$ ),  $7.01 \text{ ppm}$  ( $\text{H}_h$ ), and  $7.80 \text{ ppm}$  ( $\text{H}_k$ ). For PDODA-BPDA [Figure 2(b), top] the signal assignment is not straightforward due to the anisotropic influence of the salt group. Compared to PDODA-EDTAn, however, it can be observed the appearance of down field signals (between  $8.00$  and  $8.50 \text{ ppm}$ ) that are related to the BPDA segment, whose hydrogens are relatively more acid.

The influence of this anisotropic effect becomes clearer by observing the spectrum of FNDA-BPDA, Figure 2(c), which was performed on the imidized polymer. The signals of this spectrum could be clearly assigned as shown in the figure. By comparing FNDA-BPDA with FNDA-EDTAn the signals of the BPDA segment can be distinguished as the more acid ones [a singlet at  $8.50 \text{ ppm}$  ( $\text{H}_t$ ,  $\text{H}_p$ ), a duplet at  $8.16 \text{ ppm}$  ( $\text{H}_s$ ,  $\text{H}_u$ ), and another doublet at  $8.10 \text{ ppm}$  ( $\text{H}_r$ ,  $\text{H}_q$ ), and the signals related to FNDA as the more shielded ones. The chemical shifts of FNDA hydrogens are considerably influenced by the structure of the anhydride. For FNDA-EDTAn each signal can be clearly assigned, as shown in Figure 2(c) ( $\text{H}_1$  to  $\text{H}_6$ ). For FNDA-BPDA (completely imidized) the signals of the FNDA segment appear in a shorter range and some overlapping is observed. This is also related to the higher degree of freedom of the EDTAn segment, which can leave the hydrogens more susceptible to the magnetic field. These signal assignments are in good agreement with reports in the Refs. 19–25.

Additionally, the structure of the imidized polymers was investigated by infrared spectroscopy (Figure 3). A typical infrared spectrum of polyimides presents two carbonyl peaks of different intensities, which are related to symmetric and asymmetric stretching.<sup>19–26</sup> For BPDA-based polyimides these peaks appear at  $1776$  and  $1720 \text{ cm}^{-1}$ . By comparing the spectra in the Figure 3(a) of PDODA-BPDA (top) and FNDA-BPDA (bottom) it is possible to assign the bands for PDODA at  $1592 \text{ cm}^{-1}$ ,  $1479 \text{ cm}^{-1}$ ,  $1264 \text{ cm}^{-1}$ , and  $1170 \text{ cm}^{-1}$  [these peaks are indicated in Figure 3(a) by arrows]. The other bands are similar for both spectra and they are related to the aromatic rings and to the



**Figure 2.** (a) Structures of the polyamic salts with the respective assignment for  $^1\text{H}$  NMR spectra of (b) PDODA-EDTAn (bottom) and PDODA-BPDA (top) and (c) FNDA-EDTAn (bottom) and FNDA-BPDA (top). The signals indicated with \* are related to the solvent DMF. [Color figure can be viewed in the online issue, which is available at [wileyonlinelibrary.com](http://wileyonlinelibrary.com).]

imide group. For the EDTAn based polyimides [Figure 3(b)] there are more signals related to carbonyls ( $1694\text{ cm}^{-1}$  with a shoulder at  $1745\text{ cm}^{-1}$  and at  $1606$  and  $1660\text{ cm}^{-1}$ ). These signals are related to the carbonyls of the amide groups, indicating that a complete imidization was not achieved for these polymers with the imidization conditions used. The imidization of these EDTAn based polymers is discussed in detail later, together with the results of TGA analyses. The interpretation of the infrared bands is in agreement with reports in the Refs. 19–26.

#### Physical-Chemical and Mechanical Properties

The X-ray diffractograms of the polyimides are shown in Figure 4. PDODA-BPDA diffractogram presents sharp and defined peaks at  $15.46^\circ$ ;  $17.52^\circ$ ;  $23.04^\circ$ , and  $25.74^\circ$ . The crystal characteristics of this polymer were described in details by Srinivas et al.<sup>12</sup> The substitution of PDODA for FNDA leads to a less crystalline polyimide (FNDA-BPDA), as can be observed in its diffractogram, which presents broader peaks indicating an increase of the amorphous character. However, a peak at  $13.8^\circ$

can be observed as the one at lower diffraction angle (higher interplanar distance), which correspond to an interplanar distance of  $3.23\text{ \AA}$ . This value is higher than the one observed for PDODA-BPDA ( $2.89\text{ \AA}$  related to the peak at  $15.45^\circ$ ). This increase in interplanar distance is due to the cardo fluorene moiety, which hinders the molecular packing.<sup>27</sup> A consequence of this is that the solvent molecules can more easily penetrate between the polymer chains, resulting in FNDA-BPDA to be soluble.

Comparing PDODA-BPDA with PDODA-EDTAn diffractograms it can be observed that changing BPDA by EDTAn results in a considerable decrease in the crystallinity. This is related to the higher degree of freedom of the EDTAn segment, which allows different molecular conformations inhibiting a regular crystalline arrangement. Moreover, the imidization of PDODA-EDTAn was not complete and the presence of different segments in the polymer chain can also contribute to the decrease of the crystallinity. On the other hand, such decrease in crystallinity is not observed by comparing FNDA-BPDA and FNDA-EDTAn. In

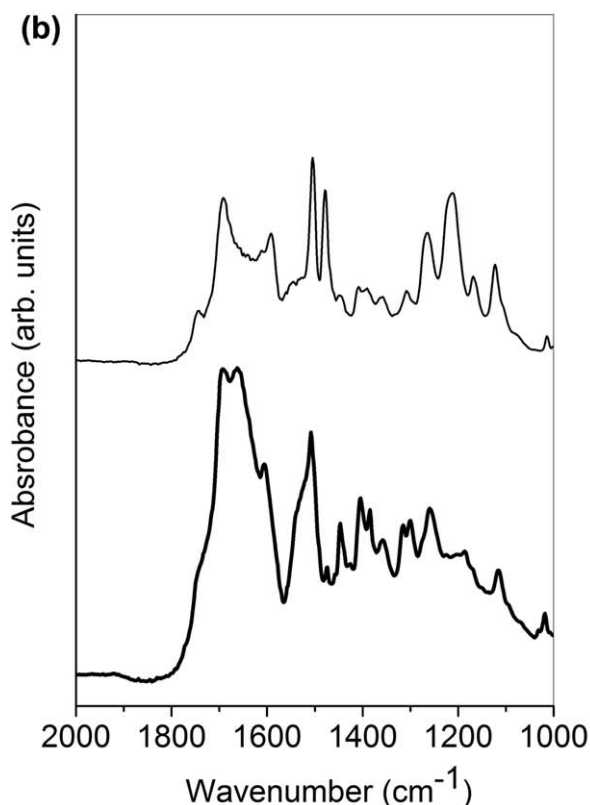
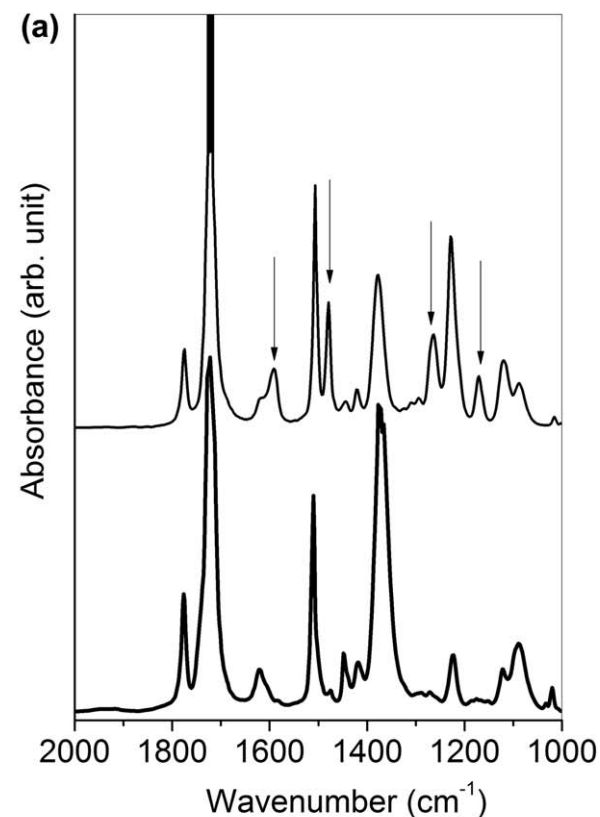


**Figure 3.** Infrared spectra of the polyimides: (a) PDODA-BPDA (top) and FNDA-BPDA (bottom); (b) PDODA-EDTAn (top) FNDA-EDTAn (bottom). The arrows indicate the signals related to the PDODA-segment.

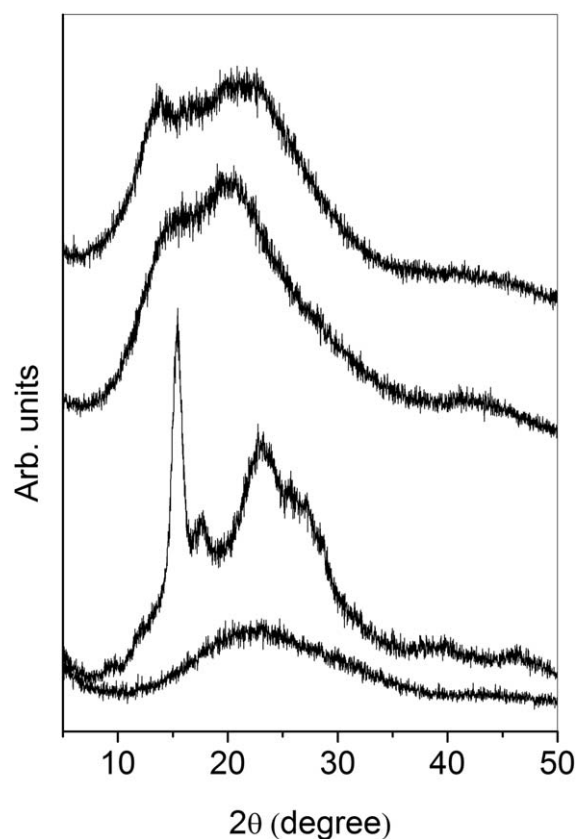


**Figure 4.** XRD pattern of for the prepared polymers. From bottom to top: PDODA-EDTAn, PDODA-BPDA, FNDA-EDTAn, and FNDA-BPDA.

this case, the diamine FNDA imposes some conformation restrictions in comparison to the flexible ether linkages in PDODA, rendering regularity to the polymer chains.

The thermal stability of the polymers was investigated by thermogravimetric analyses, which were performed first on the salts to determine the temperature range of the imidization. Figure 5(a) shows the thermogravimetric curves for the homopolymers in the salt form. For these the first mass loss step starts around 150°C and finishes at 300°C. According to the literature, this step is related to the imidization that releases water and triethylamine.<sup>15,16</sup> An average value of 23% mass loss is observed for all polymers in this stage, somewhat below the expected range of 25–30%. This suggests that a residual amount (2–7%) of salts is retained at this temperature. Above 300°C the EDTAn-based polymers completely degrade, in three distinct stages: the most intense one from 300 to 450°C, followed by another one from 450 to 620°C, which appears as a shoulder in the differential curve, and a third one above this temperature. The BPDA-based polyimides degrade in one single step after imidization, with the maximum degradation rate at 600°C.

Tests were performed to imidize the polymers at 165°C, 200°C, and at 250°C for few hours in order to determine the better compromise between temperature and treatment time for the imidization process. It was observed that even after 4 h at 250°C all polymers show a mass loss between 150°C and 300°C in thermogravimetric analyses. By treating the polymers at

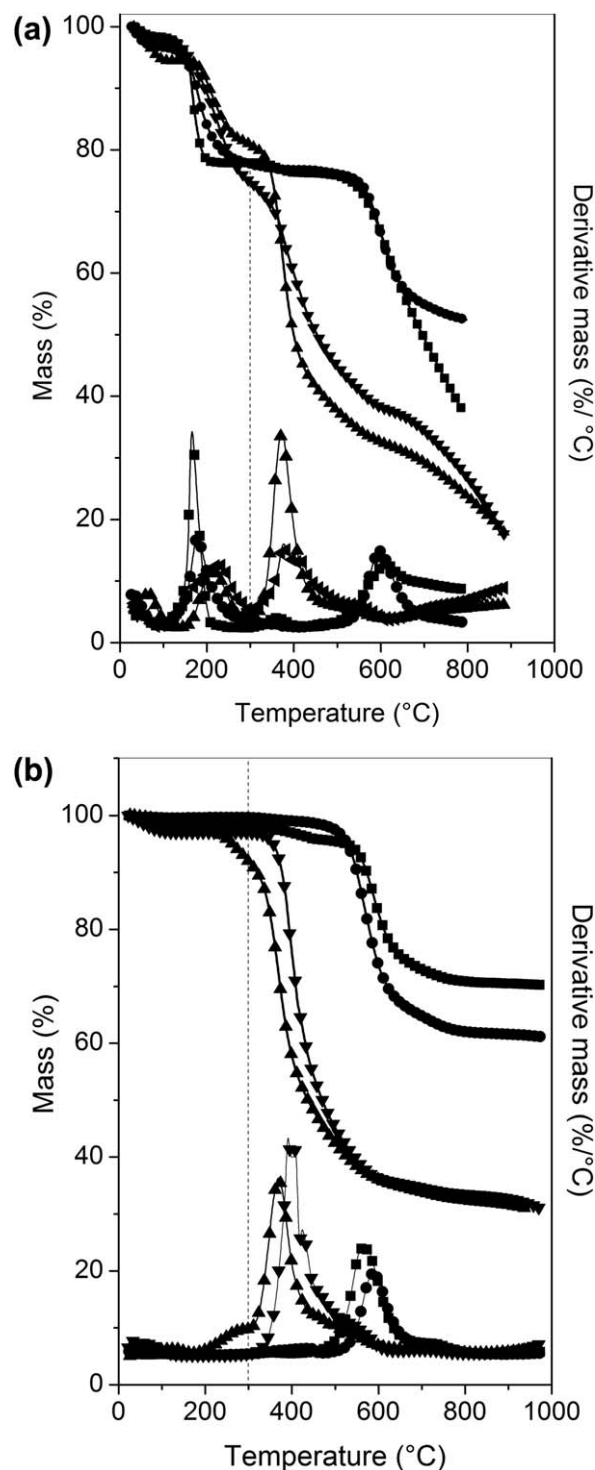


**Figure 5.** Thermogravimetric curves for (a) the polymer salts and (b) imidized polymers: PDODA-BPDA (■), FNDA-BPDA (●), FNDA-EDTAN (▼), and PDODA-EDTAN (▲).

300°C no mass loss in this range was observed (with the exception of PDODA-EDTAN, which shows 6% loss) as shown in Figure 5(b). As above this temperature the EDTAN-based polymers start to degrade, 300°C was selected as the most appropriate temperature for the thermal imidization process.

The mass loss observed between 150°C and 300°C for the imidized PDODA-EDTAN [Figure 5(b)] suggests that the complete imidization is hardly achieved as also observed in the FTIR analyses. On the other hand, FNDA-EDTAN does not show a mass loss below 300°C after imidization, despite the presence of amide signals in the infrared spectra. Nevertheless, the differential thermogravimetric curve for this polymer shows that the degradation in the second stage occurs in different steps while a single step is observed for PDODA-EDTAN. These results further suggest that a certain amount of salt is imidized at temperatures above 300°C and, in case of EDTAN's polymers, this takes place together with polymer degradation. This is corroborated by the shift in the imidization peak of the differential curve for PDODA-EDTAN in the salt and imidized form. For the salt, this peak is centered at 210°C while for the imidized polymer it appears as a shoulder at 310°C. This behavior is related to the increase in polymer rigidity as the imidization degree increases. The BPDA-based polymers also show a mass loss around 450°C, especially PDODA-BPDA, which can be related to the imidization of residual salt groups.<sup>28</sup>

The literature reports a few studies using EDTAN in the main chain of polyamic acids (polyimide precursors) and polyimides,<sup>23,26</sup> but most of these did not discuss the imidization process. Li et al.<sup>26</sup> reported that imidization of an aliphatic EDTAN polyimide could take place at 150°C. Nevertheless, considering the infrared spectra shown by the authors (which have similar bands to the ones reported in this study) we believe that a complete imidization was also not achieved. Therefore, it can be concluded that a complete thermal imidization of EDTAN-based polyimides cannot be accomplished, since temperatures above 300°C would be required, which also cause degradation of the polymer. Nevertheless, chemical imidization may be a suitable mean to completely imidize EDTAN-based polymers.

The glass transition temperature of the polyimide was determined by DSC and DMTA [Figure 6]. The  $T_g$  of EDTAN-based polyimides were obtained by DSC since their films are too brittle making the DMTA analyses impossible, while the  $T_g$  of BPDA-based polyimides were analyzed by DMTA since no clear glass transition was observed in the DSC curves. The glass transition temperatures for the EDTAN-based polyimides are 170 and 260°C for PDODA-EDTAN and FNDA-EDTAN, respectively [Figure 6(a)]. Figure 6(b) shows the loss modulus curves for the BPDA polyimides. The intense peak with maximum at 245°C is assigned to the glass transition of the PDODA-BPDA while for FNDA-BPDA even at 500°C no clear glass transition could be observed, indicating that this polymer has a  $T_g$  above 500°C (the literature reports  $T_g$  of 492°C for this polymer, based on DSC analyses<sup>27</sup>). These results show how the monomer rigidity influences the polymer thermal properties. By changing PDODA for FNDA it is possible to increase a polyimide  $T_g$  by more than 200°C. A decrease in similar magnitude is obtained by changing the dianhydride BPDA for EDTAN. Despite the high glass transition temperatures, both PDODA-BPDA and FNDA-BPDA formed flexible films by casting due to secondary relaxations, which take place around -150°C and a broad one from 0°C to 150°C.



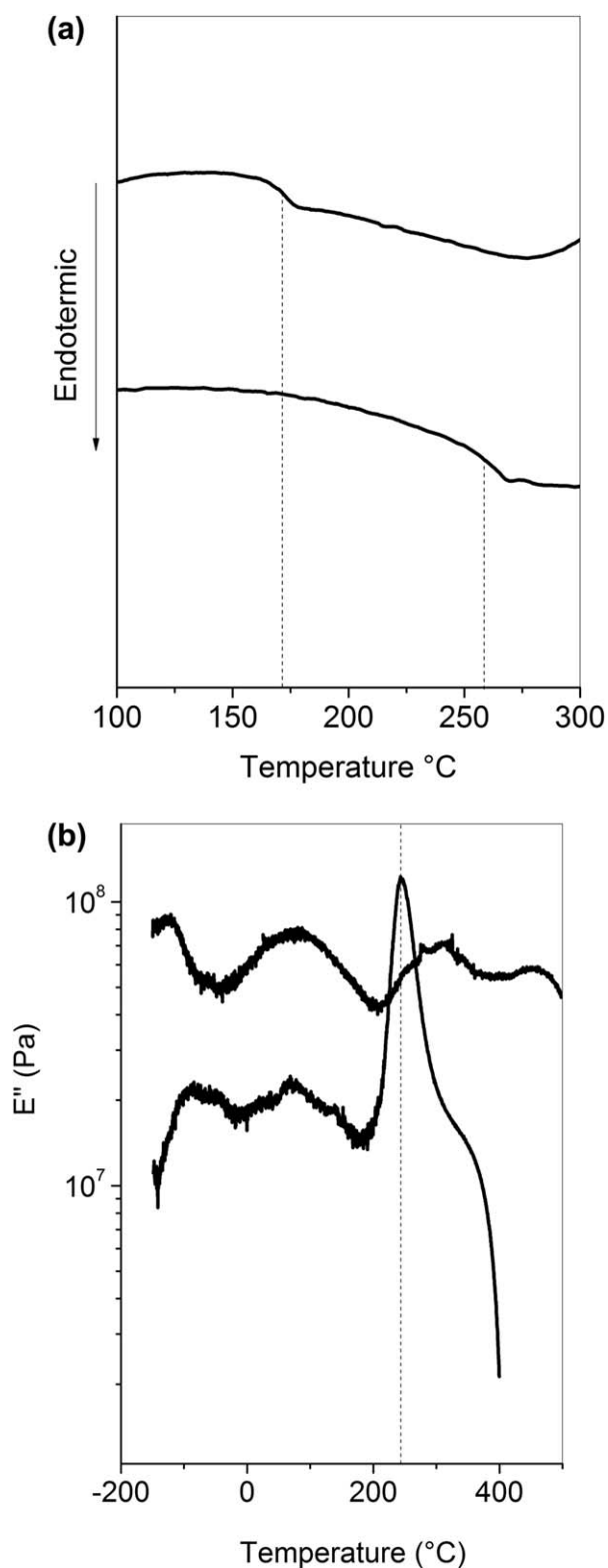


**Figure 6.** (a) DSC curves of FNDA-EDTAn (bottom) and PDODA-EDTAn (top); (b) loss modulus curves of PDODA-BPDA (bottom) and FNDA-BPDA (top).

It is important to point out that some articles in the literature report that FNDA-BPDA films are too brittle to be used as a free-standing material,<sup>14</sup> while other publications discuss

membranes of this material without mentioning any problem related to brittleness.<sup>27</sup> We observed that films of the salt precursor of this polymer are very brittle while flexible films can be prepared with the imidized polymers. Therefore, it is possible that these reports of brittleness are related to the salt or any

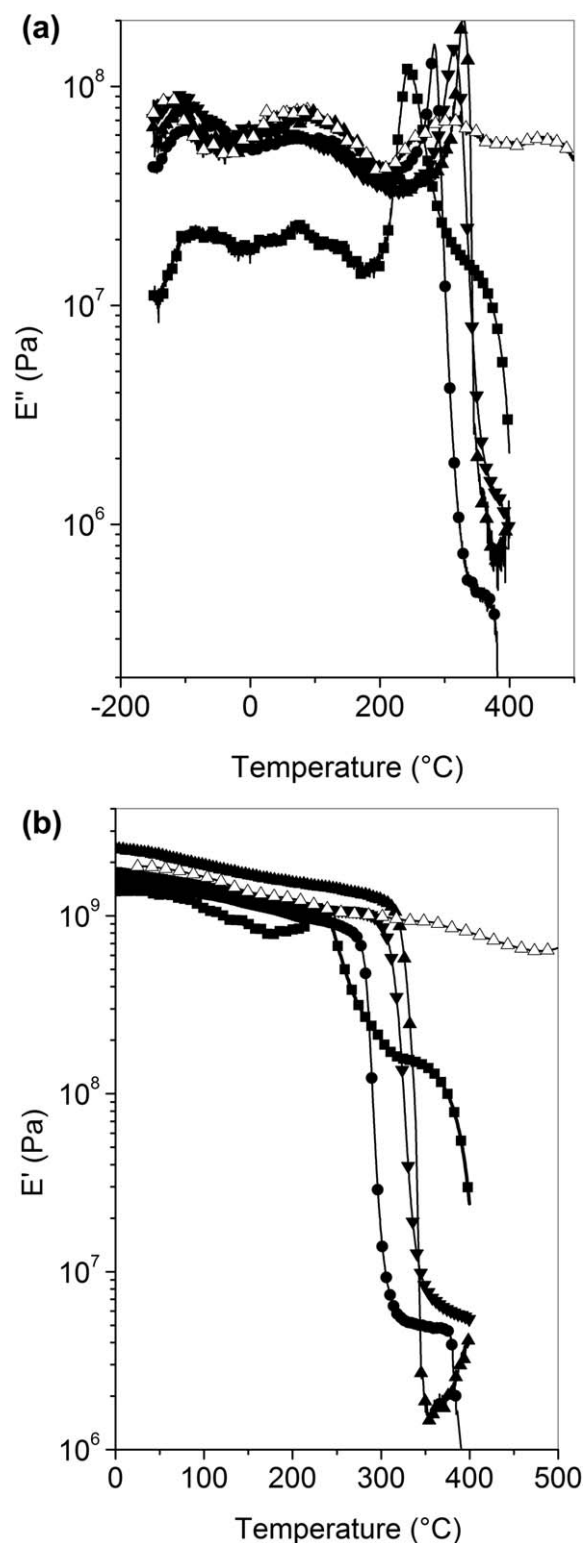


**Figure 7.** Loss (a) and storage modulus (b) for: PDODA-BPDA (■), PD20FN (•), PD40FN (▼), PD50FN (▲), and FNDA-BPDA (Δ).

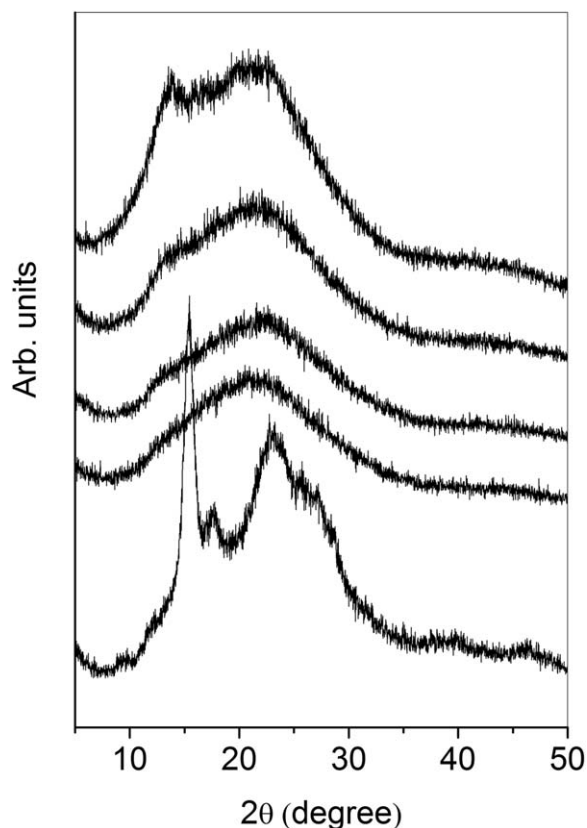


**Figure 8.** XRD pattern for PDODA-BPDA, FNDA-BPDA, and their copolymers. From bottom to top: PDODA-BPDA, PD20FN, PD40FN, PD50FN, and FNDA-BPDA.

other precursor. Besides flexibility, films of FNDA-BPDA show storage modulus close to  $10^9$  Pa at  $500^\circ\text{C}$  [Figure 7(b)], a very important property for applications as flexible substrates for circuits and memories.<sup>2</sup> Compared to results in the literature, our film maintains high storage modules in a broader temperature range.<sup>13</sup>

On the other hand EDTAn-based polymers in the salt form are flexible and become brittle after the imidization and because of

this free-standing films could not be prepared for these two polyimides. These polymers also showed high adherence to glass and Teflon® substrates.

#### Characterization of the Copolymers

Among the four synthesized homopolymers, FNDA-BPDA and PDODA-BPDA formed free-standing films with good mechanical properties. Aiming to increase the  $T_g$  and solubility of PDODA-BPDA, random copolyimides were prepared by adding FNDA to PDODA-BPDA in the amounts indicated in Table I. All of these copolyimides form flexible films and show molar masses and polydispersity in the same range as the homopolymers, as shown in Table I. These copolyimides were also characterized by  $^1\text{H}$  NMR and FTIR (results will not show in this article) and showed similar signals as the ones shown in Figures 2 and 3, respectively.

Dynamic mechanical analyses of the copolyimides show that the  $T_g$  increases gradually with the content of FNDA [Figure 7(a)], going from  $245^\circ\text{C}$  for PDODA-BPDA to  $330^\circ\text{C}$  for the copolymer with 50% of FNDA. The addition of only 20% of FNDA changes the behavior of the storage modulus significantly [Figure 7(b)]. While for PDODA-BPDA the storage modulus right after the  $T_g$  is on the order of 100 MPa, with 20% of FNDA this value falls to 1 MPa. This is related to changes in crystallinity degree. Indeed, PDODA-BPDA is a semicrystalline polymer, which forms brown opaque films, while the copolymers are predominantly amorphous (see X-ray diffractograms in Figure 8) and form transparent films with colors ranging from red to yellow (Figure 9). Sheets of PD20FN could also be prepared by hot pressing at  $350^\circ\text{C}$ .

Besides increasing the glass transition temperature, the solubility of PDODA-BPDA is also considerably influenced by the addition of FNDA. This is due to the increase in intermolecular spacing produced by the cardo fluorene moiety, as discussed previously. PD50FN showed good solubility in NMP in the imidized form, while the other copolymers only swell in the presence of this solvent. The addition of FNDA also increases the temperature of maximum degradation rate (Table II) taken as the temperature corresponding to the maximum of the peak in the differential thermogravimetric curves. For copolymers this

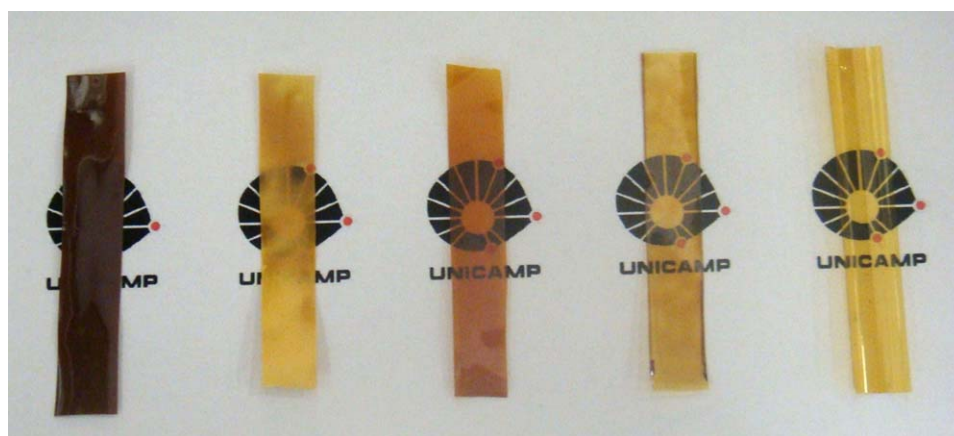


**Figure 9.** Picture of the prepared films. From left to right: PDODA-BPDA, PD20FN, PD40FN, PD50FN, and FNDA-BPDA. [Color figure can be viewed in the online issue, which is available at [wileyonlinelibrary.com](http://wileyonlinelibrary.com).]

**Table II.** Summary of General Properties

|                             | PDODA-EDTAn | FNDA-EDTAn | PDODA-BPDA | PD20FN    | PD40FN    | PD50FN    | FNDA-BPDA | Ultem®           |
|-----------------------------|-------------|------------|------------|-----------|-----------|-----------|-----------|------------------|
| Thermal properties          |             |            |            |           |           |           |           |                  |
| $T_g$ (°C)                  | 170         | 260        | 244        | 285       | 315       | 330       | >500      | 213 <sup>a</sup> |
| $T_{deg}$ (°C) <sup>b</sup> | 350         | 400        | 566        | 576       | 578       | 583       | 588       | -                |
| Mechanical properties       |             |            |            |           |           |           |           |                  |
| Modulus (GPa)               | -           | -          | 2.9 ± 0.2  | 1.8 ± 0.3 | 2.5 ± 0.2 | 2.9 ± 0.2 | 3.3 ± 0.4 | 2.0 ± 0.1        |
| UTS (MPa)                   | -           | -          | 71 ± 10    | 70 ± 9    | 80 ± 6    | 61 ± 16   | 67 ± 10   | 76 ± 5           |
| Elongation (%)              | -           | -          | 3.3 ± 0.5  | 10 ± 4    | 6 ± 1     | 2.6 ± 0.8 | 2.3 ± 0.4 | 5.2 ± 0.8        |
| Dielectric properties       |             |            |            |           |           |           |           |                  |
| $\epsilon'$ at 1 kHz        | -           | -          | 3.1        | 3.4       | 3.5       | 3.9       | 3.0       | 3.1 <sup>a</sup> |

<sup>a</sup>From Ref. 4.<sup>b</sup> $T_{deg}$ , Temperature corresponding to the maximum of the peak in the differential thermogravimetric curves.

temperature is intermediate to those of PDODA-BPDA and FNDA-BPDA

### Films Properties

As the most important end use of polyimides is as films for different applications, special attention was given in characterizing the mechanical and dielectric properties of the polyimides films. Table II shows that the polyimide films described in this study have similar or better performances in tensile strength, modulus, and elongation, as compared to the Ultem® films prepared in the same manner, with the considerable advantage of higher thermal stability. Overall, the mechanical properties of the poly-

imide films described in this study are competitive to commercially available ones described in Ref. 4. No regular trend in mechanical properties is observed with increasing amount of FNDA in the copolymers.

Figure 10 shows the dielectric constant ( $\epsilon'$ ) for the tested films with the applied frequency. It can be observed that the homopolymers (PDODA-BPDA and FNDA-BPDA) have the lowest dielectric constant (around 3.0 in the kHz frequencies). The higher dielectric constant observed for the copolyimides is probably due to their lower crystallinity degree since the molecular mobility is hindered in a crystal lattice in comparison to the same molecule in the amorphous state. Moreover, for copolyimides the dielectric constant increases progressively with the amount of FNDA and this effect is due to the higher polarizability of the FNDA segments in the copolymer chain.

The dielectric constant for the polyimides abruptly decreases at frequencies higher than  $10^4$  Hz with the exception of the copolyimide with 50 wt % of FNDA (PD50FN) for which a gradual decrease of the dielectric constant is observed in the same frequency range. This can be explained based on the relaxations time of the polymer chains. If the frequency employed in the experiments of electrochemical impedance spectroscopy is higher enough to hinder the molecular relaxations, the permanent dipoles of the macromolecules segments cannot align to the alternating electric field and the dielectric constant decreases. The dependence of the dielectric constant with the frequency observed for the PD50FN indicates that the dipoles are relatively more susceptible to align to the electric field. However, the experimental data do not allow to explain this anomalous behavior in relation with the others polyimides.

For applications such as flexible substrates for electronic circuits and solar cells, low dielectric constants are an important property. For such applications, high thermal stability is also a requirement, since high temperatures are applied during device manufacture. Among all the prepared films, FNDA-BPDA has the best properties for these applications, showing a dielectric constant lower than that of Kapton® with similar thermal stability.<sup>4</sup> On the other hand, a high dielectric constant and thermal stability are important prerequisites for high energy

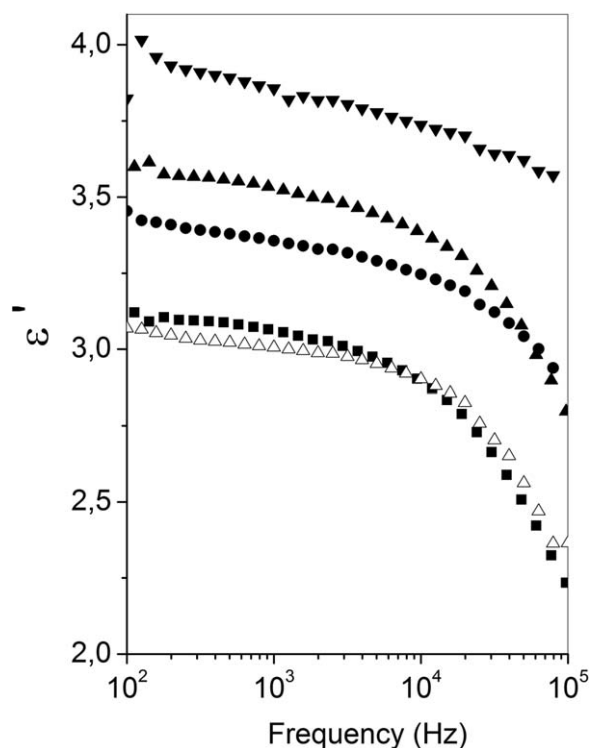


**Figure 10.** Dielectric constant obtained from impedance spectroscopy measurements: (■) PDODA-BPDA, (●) PD20FN, (▲) PD40FN, (▼) PD50FN, and (Δ) FNDA-BPDA.

capacitors for aerospace applications.<sup>29</sup> Among the prepared films, PD50FN is the one with the greatest potential in this field.

## CONCLUSIONS

After investigating the influence of the selected monomers on the physical–chemical properties of polyimides we reached the following conclusions: the flexible anhydride EDTAN segments allow a considerable decrease in  $T_g$  and thermal stability with possible decrease in the crystallinity degree. This anhydride also renders good solubility for the polymers in the salt form, including in water, but no solubility improvement was produced by this anhydride after imidization. Because of the low  $T_g$  and crystallinity degree of PDODA-EDTAN this polymer shows the best properties for the preparation of molded components. Sheets of this polymer could be prepared by hot pressing at 250°C. The monomer EDTAN does not form polyimides with good properties for the preparation of free-standing films. Nevertheless, due to the high adhesion these polyimides show on glass and Teflon® substrates, such polymers could find application as adhesives.

The gradual substitution of PDODA for the rigid FNDA diamine in a semicrystalline polyimide such as PDODA-BPDA allows a gradual increase in solubility, glass transition temperature, degradation temperature, and a decrease in crystallinity degree. The substitution of 50% renders solubility in NMP after imidization, while substitution of 20% allows the polymer to be hot pressed in sheets at 350°C. The films prepared and characterized in this study have competitive properties for applications such as substrates for flexible circuits and dielectric layers for capacitors, with superior processability, in comparison to commercially available polyimides.

## ACKNOWLEDGMENTS

The authors would like to thank Prof. C.H. Collins for manuscript revision and FAPESP for financial support (2010/02098-0 e 2010/17804-7) and a post-doctoral fellowship (2010/18268-1).

## REFERENCES

1. Cantor, B.; Grant, P.; Assender, H. *Aerospace Materials*; Taylor & Francis: London, **2001**; p 1.
2. Ling, Q.; Liaw, D.; Zhu, C.; Chan, D. S.; Kang, E.; Neoh, K. *Prog. Polym. Sci.* **2008**, *33*, 917.
3. Liaw, D.; Wang, K.; Huang, Y.; Lee, K.; Lai, J.; Ha, C. *Prog. Polym. Sci.* **2012**, *37*, 907.
4. Sroog, C. E. *Prog. Polym. Sci.* **1991**, *16*, 561.
5. Jacobs, J. D.; Arlen, M. J.; Wang, D. H.; Ounaies, Z.; Berry, R.; Tan, L.; Garrett, P. H.; Vaia, R. A. *Polymer* **2010**, *24*, 3139.
6. Deligoz, H.; Ozgumus, S.; Yalcinyuva, T.; Yildirim, S.; Deger, D.; Ulutas, K. *Polymer* **2005**, *46*, 3720.
7. Conceicao, T. F.; Scharnagl, N.; Blawert, C.; Dietzel, W.; Kainer, K. U. *Corros. Sci.* **2011**, *52*, 2066.
8. Conceicao, T. F.; Scharnagl, N.; Dietzel, W.; Kainer, K. U. *Corros. Sci.* **2010**, *52*, 3155.
9. Conceicao, T. F.; Scharnagl, N.; Dietzel, W.; Kainer, K. U.; *Corros. Sci.* **2011**, *53*, 338.
10. Ghosh, A.; Sen, S. K.; Banerjee, S.; Voit, B. *RSC Adv.* **2012**, *2*, 5900.
11. Rata, V.; Stancik, E. D.; Ayambem, A.; Pavaatareddy, H.; McGrath, J. E.; Wilkes, G. L. *Polymer* **1999**, *40*, 1889.
12. Srinivas, S.; Caputo, F. E.; Graham, M.; Gardner, S.; Davis, R. M.; McGrath, J. E.; Wilkes, G. L. *Macromolecules* **1997**, *30*, 1012.
13. Seo, J.; Cho, K.; Han, H. *Polym. Degrad. Stab.* **2001**, *74*, 133.
14. An, H.; Zhan, M.; Wang, K. *Polym. Eng. Sci.* **2011**, *51*, 1533.
15. Ding, Y.; Bikson, B.; Nelson, J. K. *Macromolecules* **2002**, *35*, 905.
16. Facinelli, J. V.; Gardner, S. L.; Dong, L.; Sensenich, C. L.; Davis, R. M.; Riffle, J. S. *Macromolecules* **2006**, *29*, 7342.
17. Araujo, A. C. V.; Oliveira, R. J.; Junior, A. S.; Rodrigues, A. R.; Machado, F. L. A.; Cabral, F. A. O.; Azevedo, W. M. *Synth. Met.* **2010**, *160*, 685.
18. Mohan, J. *Organic Spectroscopy: Principles and Applications*, 2nd ed.; Alpha Science International: Harrow; **2002**, p 1.
19. Zhang, T. M. S.; Li, Y.; Yang, F.; Gong, C.; Zhao, J. *Polym. Degrad. Stab.* **2010**, *95*, 1244.
20. Yang, C. P.; Chen, R. S.; Hung, K. S. *Polymer* **2001**, *42*, 4569.
21. Lee, T.; Park, S. S.; Jung, Y.; Han, S.; Han, D.; Kim, I.; Há, C. S. *Eur. Polym. J.* **2009**, *45*, 19.
22. Ruiz, J.; Mantecon, A.; Cadiz, V. *Polymer* **2001**, *42*, 6347.
23. Padavan, D. T.; Wan, W. K. *Mater. Chem. Phys.* **2010**, *124*, 427.
24. Saimani, S.; Kumar, A.; Dal-Cin, M. M.; Robertson, G. *J. Membr. Sci.* **2011**, *374*, 102.
25. Shang, X.; Fang, S.; Meng, Y. *J. Membr. Sci.* **2007**, *297*, 90.
26. Li, B.; Liu, T.; Zhong, W. H. *Polymer* **2012**, *52*, 5186.
27. Kazama, S.; Teramoto, T.; Haraya, K. *J. Membr. Sci.* **2002**, *207*, 91.
28. Diahm, S.; Locatelli, M. L.; Lebey, T.; Malec, D. *Thin Solid Films* **2011**, *519*, 1851.
29. Venkat, N.; Dang, T. D.; Bai, Z.; McNier, V. K.; DeCerbo, J. N.; Tsao, B. H.; Stricker, J. T. *Mater. Sci. Eng. B: ADV* **2010**, *168*, 16.